13. Nickson, R., McArthur, J. M., Shrestha, B., Kyaw-Myint, T. O. and Lowry, D., Arsenic and other drinking water quality issues, Muzaffargarh District, Pakistan. *Appl. Geochem.*, 2005, **20**, 55–68.
14. Sun, G. F., Liu, S., Li, B., Sun, X. C., Guo, X., Qian, C. and Pi, J. B., Current situation of endemic arsenicosis in China. *Environ. Sci.*, 2001, **8**, 425–434.
15. Tseng, C. H. *et al.*, Long term arsenic exposure and incidence of non insulin dependent diabetes mellitus: a cohort study in arseniasis-hyperendemic villages in Taiwan. *Environ. Health Perspect.*, 2000, **108**, 847–851.
16. Berg, M., Tran, H. C., Nguyen, T. C., Schertenleib, R. and Giger, W., Arsenic contamination of groundwater and drinking water in Vietnam: a human health threat. *Environ. Sci. Technol.*, 2001, **35**, 2621–2626.
17. Polya, D. A. *et al.*, Arsenic hazard in shallow Cambodian groundwaters. *Mineral. Mag.*, 2005, **69**, 807–823.
18. Gurung, J. K., Ishiga, H. and Khadka, M. S., Geological and geochemical examination of arsenic contamination in groundwater in the Holocene Terai Basin, Nepal. *Environ. Geol.*, 2005, **49**, 98–113.
19. Datta, D. V. and Kaul, M. K., Arsenic content of drinking water in villages in northern India: a concept of arsenicosis. *J. Assoc. Phys. India*, 1976, **9**, 599–604.
20. Garai, R., Chakraborty, S., Dey, B. and Saha, K. C., Chronic arsenic poisoning from tube-well water. *J. Indian Med. Assoc.*, 1984, **82**, 34–35.
21. Chakraborti, D. *et al.*, Groundwater arsenic contamination and its health effects in the Ganga–Meghna Brahmaputra plain. *J. Environ. Monit.*, 2004, **6**, 74–83.
22. Shah, B. A., Role of quaternary stratigraphy on arsenic contaminated groundwater from parts of Middle Ganga Plain, UP–Bihar, India. *Environ. Geol.*, 2008, **53**, 1553–1561.
23. Singh, A. K., Arsenic contamination in the groundwater of North Eastern India. In Proceedings on National Seminar on Hydrology, Roorkee, 22–24 November 2004.
24. Chakraborti, D. *et al.*, Groundwater arsenic contamination in Manipur, one of the seven North-Eastern Hill states of India: a future danger. *Environ. Geol.*, 2008, **56**, 381–390.
25. Shah, B. A., Arsenic in groundwater from parts of Barak Valley, Chachar and Karimganj districts, Assam. *Indian J. Geol.*, 2007, **79**, 59–62.
26. Shah, B. A., Groundwater arsenic from parts of Barak Valley, Assam, North-East India. *Mineral. Mag.*, 2010 (submitted).
27. WHO, Guideline for drinking water quality. Recommendations, Geneva, 1993, vol. 1, 2nd edn.
28. Bureau of Indian Standards (BIS). Indian Standard: Drinking Water. Specification (first revision), Amendment No. 2, New Delhi, September 2003.
29. Kumar, G., Khanna, P. C. and Prasad, S., Sequence stratigraphy of the foredeep and evolution of the Indo-Gangetic plain, Uttar Pradesh. *Geol. Surv. India Spl. Pub.*, 1996, **21**, 173–207.
30. Srivastava, P., Singh, I. B., Sharma, M. and Singhvi, A. K., Luminescence chronometry and Late Quaternary geomorphic history of the Ganga Plain, India. *Palaeogeogr. Palaeoclimatol. Palaeoecol.*, 2003, **197**, 15–41.
31. Singh, I. B., Late Quaternary history of the Ganga Plain. *J. Geol. Soc. India*, 2004, **64**, 431–454.
32. Williams, M. A. J. and Clarke, M. F., Late Quaternary environments in north-central India. *Nature*, 1984, **308**, 633–635.
33. Gasse, F. *et al.*, A 13,000 year climate record from western Tibet. *Nature*, 1991, **353**, 742–745.
34. Das, S., A note on prospecting of Amjhore pyrite, Rohtas district, Bihar with discussion on the origin of the deposits. *Indian Miner.*, 1977, **31**, 8–22.
35. Raghunandan, K. R., Dhruva Rao, B. K. and Singhal, M. L., Exploration for copper, lead and zink ores in India. *Bull. Geol. Surv. India, Ser. A. Econ. Geol.*, 1981, **47**, 125–128.
36. Mishra, S. P. *et al.*, Arsenic incidence in Son valley gold belt. In Symposium on Earth Sciences in Environmental Assessment and Management, invited papers and abstracts, Lucknow (eds Shanker, R. *et al.*), Geological Survey of India, 1996, pp. 163–164.
37. Harvey, C. H. *et al.*, Arsenic mobility and groundwater extractions in Bangladesh. *Science*, 2002, **298**, 1602–1606.
38. Lovley, D. R. and Chapelle, F. H., Deep subsurface microbial processes. *Rev. Geophys.*, 1995, **33**, 365–381.
39. Saunders, J. A., Pritchett, M. A. and Cook, R. B., Geochemistry of biogenic pyrite and ferromanganese coatings from a small watershed: a bacterial connection? *Geomicrobiol. J.*, 1997, **14**, 203–217.
40. Islam, F. S., Gault, A. G., Boothman, C., Polya, D. A., Charnock, J. M., Chatterjee, D. and Lloyd, J. R., Role of metal-reducing bacteria in arsenic release from Bengal delta sediments. *Nature*, 2004, **430**, 68–71.

ACKNOWLEDGEMENTS. I thank School of Environmental Studies, Jadavpur University for arsenic and iron analyses. The financial support from DST, SERC Fast Track Young Scientist Scheme and CSIR Scientists' Pool Scheme is gratefully acknowledged.

Received 2 June 2009; revised accepted 15 April 2010

Defining optimum spectral narrow bands and bandwidths for agricultural applications

S. S. Ray[1], Namrata Jain[1], Anshu Miglani[1], J. P. Singh[2], A. K. Singh[3], Sushma Panigrahy[1] and J. S. Parihar[1]

[1]Space Applications Centre, ISRO, Ahmedabad 380 015, India
[2]Central Potato Research Station, Jalandhar 144 003, India
[3]Indian Agricultural Research Institute, New Delhi 110 012, India

In this study, an attempt was made to define the optimum set of spectral narrowbands and the required bandwidth for agricultural applications. Spectral observations were collected using ASD handheld spectroradiometer (325–1075 nm) from major *kharif* (rainy) and *rabi* (winter) season crops, two different soil types and crops under different agronomic treatments. To identify best bands, a stepwise discriminant analysis (SDA) was carried out for each data set. Aggregating the bands selected from individual SDA, 13 optimum narrow bands were identified for crop and soil assessment. To find optimum bandwidth, the measured reflectance was aggregated to different bandwidths (3, 5, 10, 15, 20, 25 and 30 nm). The reflectance values at different wavelength regions were compared with the original spectra using root mean square error. It was found that the optimum bandwidth required for crop discrimination differed for different wavelength regions.

*For correspondence. (e-mail: ssray@sac.isro.gov.in)

Keywords: Agriculture, bandwidth, hyperspectral, narrow band, stepwise discriminant analysis.

CONVENTIONAL remote sensing is based on the use of several rather broadly defined spectral regions, whereas hyperspectral remote sensing is based on the examination of many narrowly defined spectral channels[1]. In agriculture, hyperspectral remote sensing data has potential in crop stress detection[2], biophysical parameter retrieval[3], soil type discrimination[4] and soil properties quantification[5]. Because hyperspectral data comes with large number of bands, it is difficult to analyse such high dimensional data. It has also been shown that this data has high redundancy and 96% of the variability in the data could be explained using four principal components derived from 76 bands[6]. Keeping this in view, it is essential to define an optimum smaller set of narrow bands that are specific for various agricultural applications.

Apart from this, hyperspectral spectra are generally noisier as compared to the controlled laboratory situation. This is because their narrow bandwidth can only capture very little energy that may be overcome by the self-generated noise inside the sensors. Moreover, Sun's variable illumination greatly reduces incoming signal. Figure 1 shows spread of noise over the spectrum. Therefore, it is necessary to smoothen the reflectance spectra collected in the fields with handheld spectrometer or from remotely sensed images before analysis. Several requirements have to be met while selecting an optimal bandwidth for the hyperspectral data. The absorption feature should be preserved, while the wavelength position of the local minima or maxima as well as inflection points should not move. It means that the ability to resolve fine spectral details and the noise removal capacity should be well-optimized to minimize disturbances to original spectral data.

Keeping this in view, this study was carried out to define an optimum set of narrow bands and the optimum bandwidth for hyperspectral data utilization in agriculture.

To determine the optimum narrow bands a large number of spectral observations were collected, representing the wide variability existing in agriculture. Observations were collected from different locations such as experimental farms of Indian Agricultural Research Institute (IARI), New Delhi (77.20°E long. and 28.63°N lat.); Punjab Agricultural University (PAU) Research Station, Bathinda, Punjab (74.58°E long. and 30.17°N lat.) and Central Potato Research Station (CPRS), Jalandhar, Punjab (75.32°E long. and 31.16°N lat.). The study included, the major *kharif* (rainy) and *rabi* (winter) season crops like, rice, wheat, maize, pearl millet, gram, soybean, mustard and cotton. Different agronomic treatments such as irrigation, fertilizers, variety and date of sowing were also studied. Soils with significantly different nutrition parameters were included in the analysis (Table 1). There were total six sets of observations.

Spectral reflectance for soil and crop was collected using a 512-channel spectroradiometer[7] with a range of 325–1075 nm. The instrument acquired hyperspectral data at the spectral resolution of 3 nm. But by sampling, the instrument delivers data with 1 nm interval. Gathering spectra at a given location involved optimizing the integration time (typically set at 17 ms) providing foreoptic information, recording dark current, collecting white reference reflectance and obtaining the target reflectance. The target reflectance is the ratio of energy reflected off the target (e.g. crop) to energy incident on the target (measured using $BaSO_4$ white reference). Since the dark current varies with time and temperature, it was gathered for each integration time (virtually new for each plot).

Reflectance measurements were made about 1 m above the crop canopy/soil surface with the sensor facing the target and oriented normal to the plant. The reflectance measurements were collected for soil and crop using 25° field-of-view (FOV). This FOV was selected, so that at least 40 cm diameter crop region will be covered when the instrument is kept 1 m above canopy. The readings were taken on cloud-free days at around solar noon-time; while taking the observations care was taken not to cast shadow over the area being scanned. A total of 10–15 spectral reflectance profile observations were collected for each crop/treatment/soil type. For viewing, analysing and exporting the spectral data, a window-based software View Spec Pro was used.

The reflectance profile contained spectral wavelengths from 325 to 1075 nm with 1 nm interval. However, previous studies[8,9] have shown that wavebands in immediate neighbourhood of one another provide similar information, hence becoming redundant. Given these facts, we have averaged the spectral data over 10 nm thus reducing the number of data points to 75 wavelengths. There are various methods to compress the data from 1 to 10 nm. However, we did simple averaging, assuming a square wave spectral response function within 10 nm range. We found that within any 10 nm range, the coefficient of variation of reflectance was less than 2% (ref. 6). Hence an average can appropriately represent the reflectance values of that range.

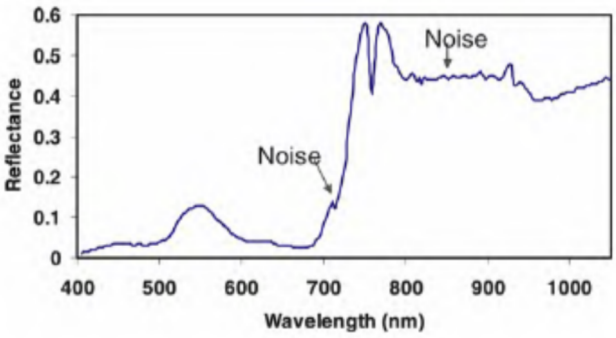

Figure 1. A field spectrum of rice crop with handheld spectroradiometer.

Table 1. Data set for optimum narrowband selection

Discrimination set	Targets	Location
Crops (*kharif*)	Rice, maize, cotton, soybean, pearlmillet	IARI, New Delhi
Crops (*rabi*)	Chickpea, mustard, wheat	IARI, New Delhi
Crop variety	15 wheat varieties	IARI, New Delhi
Crop stage	Mustard two stages	IARI, New Delhi
Crops (date of sowing)	Two dates of sowing of cotton	PAU Farm, Bathinda, Punjab
Crop treatment (irrigation)	Three irrigation treatments in potato crop	CPRS Farm, Jalandhar, Punjab
Crop treatment (nitrogen)	Five nitrogen treatments in rice crop	CPRS Farm, Jalandhar, Punjab
Crop treatment (phosphorus)	Five phosphorus treatments in rice crop	CPRS Farm, Jalandhar, Punjab
Soil type	Four fields with varying soil types	CPRS Farm, Jalandhar, Punjab

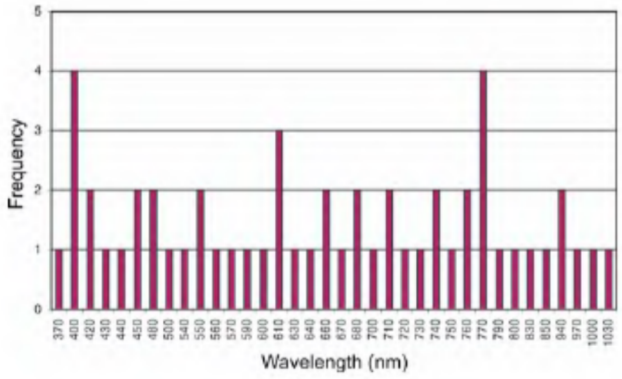

Figure 2. Frequency of occurrence of various bands in different sets of stepwise discriminant analysis.

To get the best narrow band indices for crop discrimination under different nitrogen treatments, the stepwise discriminant analysis (SDA) was carried out. Wilks' Lambda is the test statistic preferred for multivariate analysis of variance (MANOVA) and is found through a ratio of the determinants. Wilks' lambda (Λ) is given by[10]

$$\Lambda = \frac{|S_{\text{effect}}|}{|S_{\text{effect}}| + |S_{\text{error}}|},$$

where S is a matrix which is also known as sum of squares (SS) and cross-products (SSCP).

Wilks' lambda is a multivariate test of significance and ranges within 0 to 1. The values close to 0 indicating the group means are different and values close to 1 indicating the group means are not different and 1 indicates all means are the same. The SDA was carried out using SPSS 10.0.5 (ref. 11).

The spectral resolution of ASD handheld spectroradiometer is 3 nm, though it provides data at every 1 nm through resampling. To select the optimum bandwidth observations were collected from rice crop with five different nitrogen treatments grown in the CPRS farm, Jalandhar. This observation target was selected because the nitrogen treatments had generated large variability in the rice crop. The leaf area index (LAI) varied from 0.4 to 1.7 whereas the total chlorophyll content (mg/g leaf) varied from 2.51 to 4.18. The data was integrated to 3, 5, 10, 15, 20, 25 and 30 nm width using ViewSpec software, which comes with spectroradiometer. The reflectance curves and first derivative of reflectance were prepared for each bandwidth. The derivative reflectance spectra amplify the changes in the original reflectance spectra. The reflectance values were compared with 3 nm spectra at different reflectance/absorption peaks. Root mean square error (RMSE) at each level of integration from the 3 nm was also calculated for different regions of the spectrum.

The final results of SDA, showing the wavelengths selected for discrimination and corresponding multivariate statistics are shown in Table 2. When we compare the statistics, it can be found that there was best discrimination among cotton crop under two dates-of-sowing followed by soil types and then crop types. The lowest discrimination was between rice crops with different phosphate fertilizer treatments.

By combining all these wavelengths, we could find 36 unique wavelengths. These wavelengths were categorized by the frequency of their occurrence in different sets of SDA (Figure 2). We selected only those bands which have frequency of two or more. The study could identify 13 optimum bands in VNIR (400–1050 nm) region for crop and soil assessment, by combining the bands selected from individual discriminant analysis. These included bands in ultraviolet (2), blue (2), green (1), red (3), red edge (2), NIR (2) and moisture sensitive NIR (1) region. The importance of these bands is shown in Table 3.

The reflectance spectra and their first derivative integrated to different bandwidths, for rice crop, are presented in Figure 3. These curves are plotted with offset for better viewing. Hence, the curves need to be studied with respect to their pattern, rather than reflectance values. It showed that the 3 nm data is highly noisy followed by 5 nm data. The noise reduction started from 10 nm. However, when it went up to 20–30 nm level of integration, many of the absorption features were getting smoothened, as can be seen in 700–750 nm range in 1st derivative spectra.

Table 2. Results of stepwise discriminant analysis on different datasets

Source of variation	Wavelengths selected	Wilks' lambda	*F* value
Rabi season crops (4)	400, 450, 480, 550, 660, 680	0.000	85.5
Kharif season crops (5)	400, 420, 450, 500, 550, 590, 600, 610, 670, 660, 710, 730, 740, 760, 830, 940	0.001	86.380
Wheat varieties (15)	370, 940, 770, 750, 1030	6.32E-05	
Mustard stages (2)	400, 430, 480, 610	0.065	53.9
Cotton – dates-of-sowing (2)	560, 700	0.001	1568.2
Rice: nitrogen treatments (5)	400, 440, 570, 710, 740, 760, 770, 800, 930, 970	0.001	22.5
Rice: phosphorus treatments	640, 680	0.701	3.451
Potato: irrigation treatments*	540, 610, 630, 700,1000	0.172	8.16
Soil types (4)	420, 720, 770, 790, 850	0.000	319.6

*Source: Ray *et al.*[6].

Table 3. Importance of the selected bands for agricultural applications

Band	Importance
400, 420	Chlorophyll *a* absorption peak at 430 nm, carotenoid shoulder at 425 nm
450, 480	Chlorophyll *b* absorption peak at 460 nm and carotenoid absorption peaks at 455 and 480 nm
550	Green reflectance peak, maximum reflectance in the visible spectrum, anthocyanin absorption peaks at 530 nm
610	Influenced by chlorophyll *b* absorption peak at 640 nm
660	Chlorophyll *a* absorption peak
680	Greatest crop-soil contrast. Chlorophyll absorption maxima
710, 740	Red edge
760, 770	NIR reflectance
940	Influenced by water absorption at 970 nm and maximum reflectance region of the NIR spectrum at 920

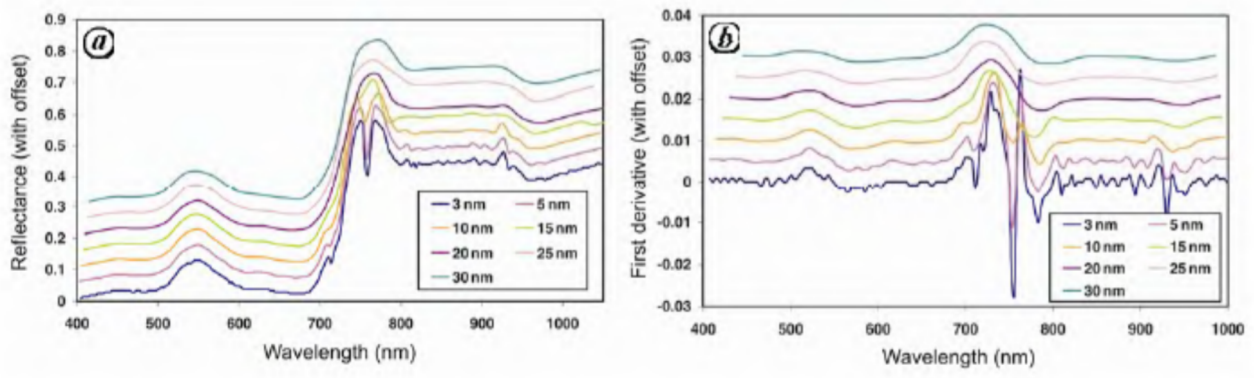

Figure 3. Spectral profile of (***a***) reflectance and (***b***) its first derivative for rice crop with N dose 180 kg/ha at different levels of integration (N.B. The curves are presented with offsets for proper viewing. Curves need to be studied for their pattern but not for reflectance values).

Comparison of the reflectance of different peaks (Table 4) showed that with a higher level of integration the reflectance decreased at green and NIR peaks, and increased at red absorption peak. However, up to 10 nm integration, in the green peak, reflectance difference remained within 2% of 3 nm bandwidth. It was found that, in the red absorption peak, the reflectance difference was low (less than 5% of 3 nm spectrum) up to 10 nm integration level. In green and NIR reflectance peaks, the reflectance difference was low up to 15 nm integration level.

RMSE calculated for all levels of integration in comparison to 3 nm data, showed that for 700–800 nm region, which includes the red edge, finer the resolution lower the RMSE (Figure 4). Because this region is very crucial for crop stress studies finer bandwidth is required. For 600–700 and 800–900 nm region, there was no change in RMSE, till 15 nm bandwidth. For 400–500 nm and 900–1000 nm region the RMSE does not change up to 25 nm integration. This is because near uniform reflectance in this region, as can be seen from the derivative spectrum. Earlier studies[12] also concluded that different bandwidths were found to be optimum for different regions in the spectrum. The bandwidths specified by them ranged from 4 nm in red region to 70 nm in NIR region.

Table 4. The reflectance difference of smoothened spectra from the original 3 nm spectrum (for nitrogen treatment 180 kg/ha)

	Bandwidth (nm)						
Parameters	3	5	10	15	20	25	30
At green maximum							
Reflectance (%)	13.0	13.0	12.8	12.5	12	11.8	11.3
Difference from 3 nm	–	0.0	–0.2	–0.5	–1.0	–1.2	–1.7
At red minimum							
Reflectance (%)	2.5	2.5	2.6	2.7	2.5	2.75	2.9
Difference	–	0.0	0.1	0.2	0.0	0.25	0.4
At NIR maximum							
Reflectance (%)	58.0	57.0	56.0	55.0	52.0	52.0	53.0
Difference	–	–1.0	–2.0	–3.0	–6.0	–6.0	–5.0

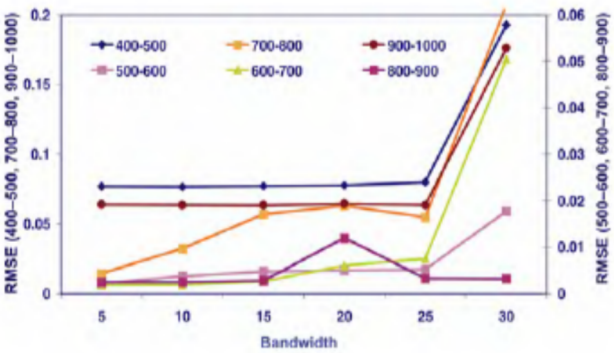

Figure 4. Root mean square error of reflectance at different wavelength regions with different band integrations.

Thus, the optimum bandwidth required for crop stress discrimination differed for different wavelength regions. It was required to have narrow bandwidth (5–10 nm) in red edge and early NIR region. In 500–700 and 800–900 nm regions, bandwidth up to 25 nm was found to be optimum.

This study was carried out to find out the optimum set of narrow bands and required bandwidth for agricultural applications. This study was particularly important in view of Indian Space Programme envisaging launching of a space-borne hyperspectral sensor in the near future. The study established 13 optimum narrow bands in the 400–1050 nm region for crop separation, crop stress discrimination and soil variability analysis. It was also observed that the required bandwidth for agricultural applications differed in different spectral regions. However, the study, may not be a conclusive one. This is because we have taken observations from a large number of agricultural targets, but many crops such as flowers and fruit crops have not been accounted for which may have typical spectral behaviour. Also, there is a need to extend this study to analyse the band specification required for biophysical parameter retrieval.

1. Campbell, J. B., *Introduction to Remote Sensing*, Taylor and Francis, London, 1996.
2. Carter, G. A., Ratios of leaf reflectance in narrow wavebands as indicators of plant stress. *Int. J. Remote Sensing*, 1994, **15**, 697–703.
3. Haboudane, D., Miller, J. R., Pattey, E., Zarco-Tejada, P. J. and Strachan, I. B., Hyperspectral vegetation indices and novel algorithms for predicting green LAI of crop canopies: modeling and validation in the context of precision agriculture. *Remote Sensing Environ.*, 2004, **90**, 337–352.
4. Palacios-Orueta, A. and Ustin, S. L., Remote sensing of soil properties in the Santa Monica Mountains I. Spectral analysis. *Remote Sensing Environ.*, 1998, **65**, 170–183.
5. Suk, Y. H., Sudduth, K. A., Kitchen, N. R., Drummond, S. T., Palm, H. L. and Wiebold, W. J., Estimating within field variations in soil properties from airborne hyperspectral images. In Pecora 15/Land Satellite Information IV/ISPRS TC I/FIEOS 2002 Conference Proceedings, 2002.
6. Ray, S. S., Das, G., Singh, J. P. and Panigrahy, S., Evaluation of hyperspectral indices for LAI estimation and discrimination of potato crop under different irrigation treatments. *Int. J. Remote Sensing*, 2006, **27**, 5373–5387.
7. FieldSpec®Pro, User's Guide Manual Release, Analytical Spectral Devices Inc., Boulder, Co, USA, 2000.
8. Thenkabail, P. S., Enclona, E. A., Ashton, M. S. and Van Der Meer, B., Accuracy assessments of hyperspectral waveband performance for vegetation analysis applications. *Remote Sensing Environ.*, 2004, **91**, 354–376.
9. Broge, N. H. and Leblanc, E., Comparing predictive power and stability of broad-band and hyperspectral vegetation indices fro estimation of green leaf area index and canopy chlorophyll density. *Remote Sensing Environ.*, 2000, **76**, 156–172.
10. Green, P. E. and Caroll, J. D., *Analyzing Multivariate Data*, The Dryden Press, Illinois, 1978, p. 519.
11. SPSS 1999, SPSS for Windows Release 10.0.5, SPSS Inc., 27 November 1999.
12. Thenkabail, P. S., Smith, R. B. and Pauw, E. D., Hyperspectral vegetation indices and their relationships with agricultural crop characteristics. *Remote Sensing Environ.*, 2000, **71**, 158–182.

ACKNOWLEDGEMENTS. We thank Dr R. R. Navalgund, Director, Space Applications Centre for encouragement, critical evaluation of the work and suggestions. We also thank Dr S. K. Pandey, Director, Central Potato Research Institute, Shimla for facilitating the required fieldwork at Central Potato Research Station, Jalandhar.

Received 2 June 2008; revised accepted 20 April 2010